Supporting information for

Uncovering the Contribution of Microchannel Deformation to Impedance-based Flow Rate Measurements

Pengfei Niu, Brian J. Nablo, Kiran Bhadriraju and Darwin R. Reyes*

Engineering Physics Division, Physical Measurement Laboratory, National Institute of Standards and Technology, MD, USA

*Corresponding author: darwin.reyes@nist.gov

Table of Contents

Figure S1. Ion distribution between two electrodes (a) and the corresponding simplified equivalent electrical circuit (b).

When an electrical potential is applied to an electrode in contact with an electrolyte solution, it induces the separation of ions at the electrode's interface, forming an electrical double layer. The net charge of the double layer at the electrode's surface is equal and opposite to the surface charge needed for neutralization (Fig.S1(a)). When there is no redox reaction occurring in solution, the electrical double layer can be viewed as a capacitor. So the equivalent electrical circuit between two electrodes can be considered as a capacitor in series with a resistor (Fig.S1(b)).

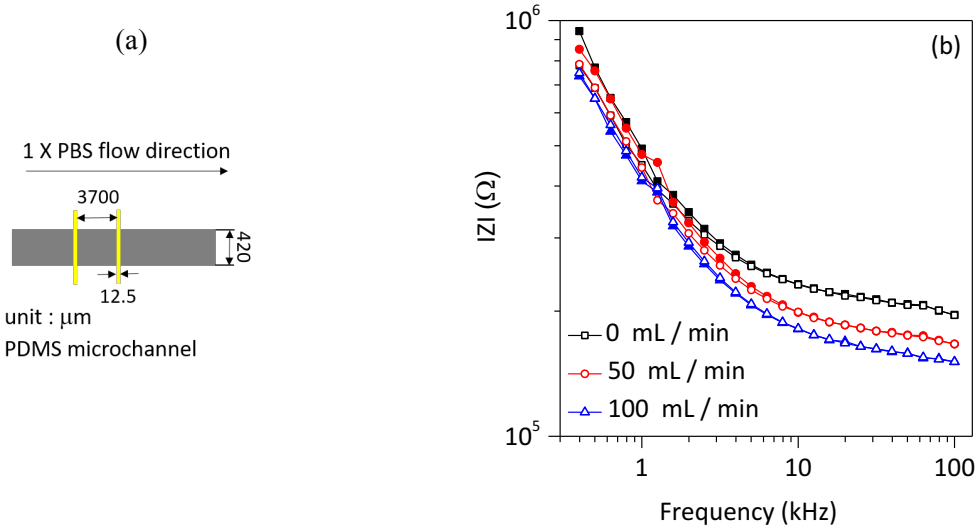

Figure S2. (a) Top view of a pair of electrodes and flexible PDMS microfluidic system employed for impedance measurements of 1X PBS solution. (b) Electrical complex impedance of 1X PBS vs. frequency measured on a pair of electrodes located near the microchannel inlet under a flow rate of 0 μL/min - square, 50 μL/min - round and 100 μL/min - triangle at two different days. Solid and open symbols represent results obtained on two different days.

The reproducibility of impedance measurements varies with frequency. At frequencies in which the solution resistance dominates the total impedance, the measurements are much more reproducible than those at lower frequencies (Fig.S2).

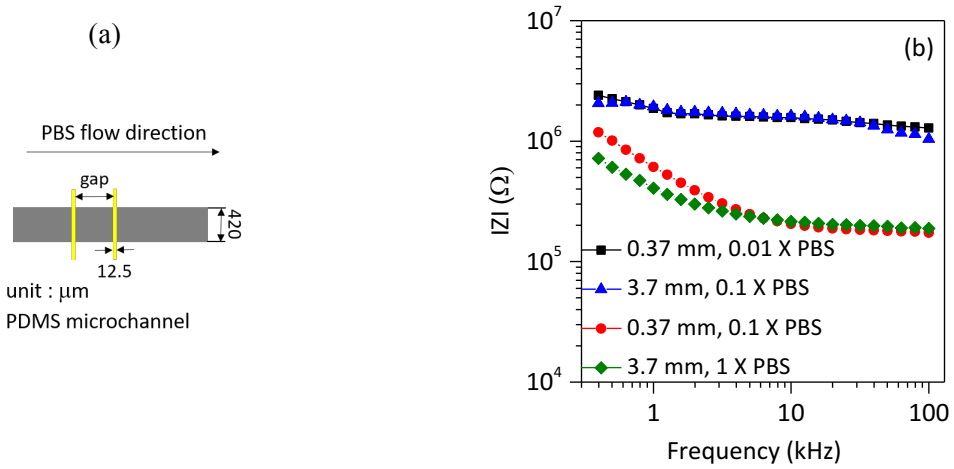

Figure S3. (a) Top view of the pair of electrodes and flexible PDMS-based microfluidic system employed for impedance measurements of 0.001X, 01X and 1X PBS solutions. (b) The electrical complex impedance vs. frequency of PBS solutions at a flow rate of 10 μL/min measured on electrodes with gap distances of 0.37 mm and 3.7 mm, respectively. The electrode pair is placed near the inlet of the microchannel.

Figure S3 shows the effect of different electrode gaps and the solution's conductivity in the electrical impedance measurement. Based on the equation $R=\rho \cdot L/S$, the solution resistance is proportional to its electrical resistivity (ρ) and gap distance (L). Comparing the impedance measured in 1X PBS and 0.1X PBS using the electrodes with a gap of 3.7 mm, and in 0.1X PBS and 0.01X PBS using the electrodes with a gap of 0.37 mm, the solution-resistance-dominant impedance increases at similar scale factors as the increase in ρ or L.

Additionally, when $\rho \cdot L$ is the same, the solution-resistance-dominant impedance between the two electrodes is nearly the same as well, as demonstrated by the sample pairs plotted as the "black and blue" symbols as well as the "red and green" symbols shown in Fig.S3. Consequently, similar sensing performance to solutions of different electrical resistivity could be achievable by varying the electrodes gap.

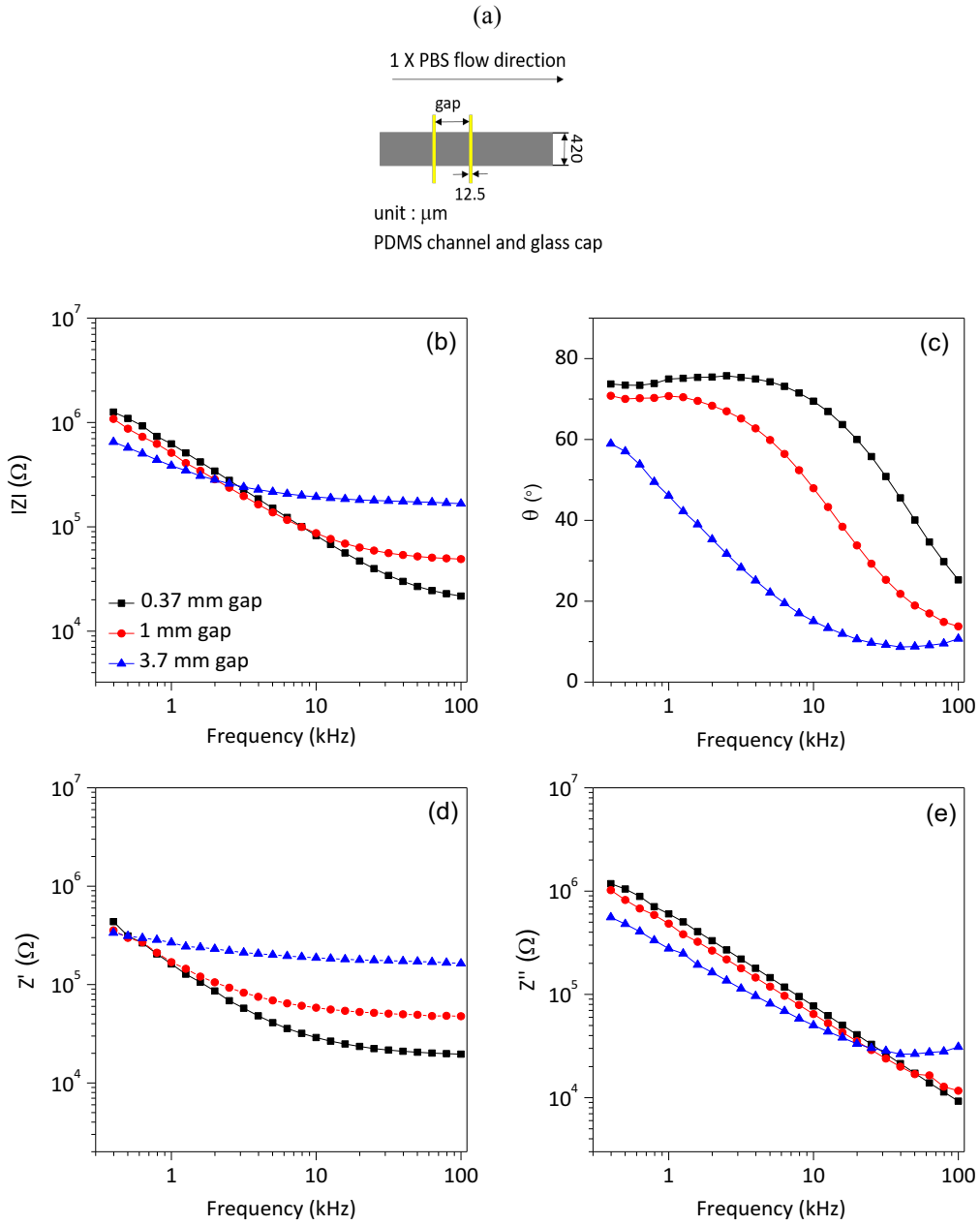

Figure S4. (a) Top view of the pair of electrodes near the microchannel inlet and flexible PDMS-based microfluidic system employed for impedance measurements in 1X PBS solution using different gaps between the electrodes. (b), (c), (d) and (e) are complex, phase angles, real and imaginary impedances of electrical impedance vs. frequency of 1X PBS solutions at a flow rate of 10 μL/min measured on electrode pairs with gap separations of 0.37 mm, 1 mm and 3.7 mm, respectively.

Widening the gap separation between electrodes increases the electrical impedance. The impact on impedance is observed mainly on its real part (Fig.S4).

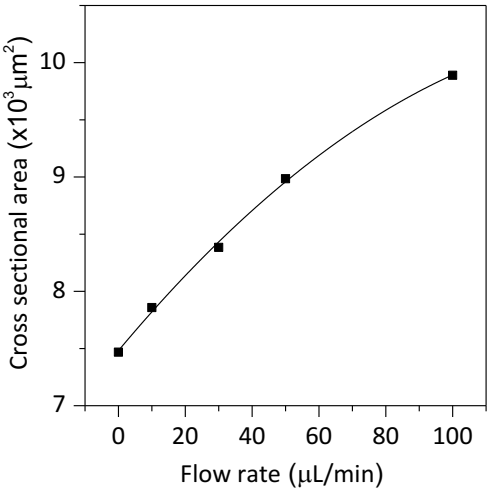

Figure S5. Variation of cross-sectional area vs. volumetric flow rate at 5.6 mm away from the channel inlet.

At a fixed position in a flexible PDMS microfluidic channel, when flow rate increases, the cross-sectional area of the channel increases. However, the increase in the cross-sectional area tapers off as we move further away from the inlet (i.e. the slope of the curve decreases). A curve with this behavior can be fitted with a 2-order polynomial. This plot explains the observed results that show that a change in electrical impedance is larger at the front end of the channel and then gradually decreases as the distance from the inlet increases, as seen in Fig.3 and Fig.7.

In flexible PDMS microfluidic systems, the cause of variation in electrical impedance is from the flow-induced microchannel deformation. To further confirm our findings, rigid SU8 film microchannels were sandwiched between two pieces of glass substrates. One of the glass substrates contains a pair of gold electrodes facing the bottom side of the channel.

We made the geometry of the SU8 microchannels and the pair of electrodes the same as those used in the PDMS microfluidic devices. The flow rate was raised up to 500 µL/min, no change in electrical impedance with the increase in flow rate of 1X PBS was observed. We stopped increasing the flow rate further to avoid breaking the bonding between SU8 film and glass substrate. However, the applied flow rate (up to 500 µL/min) to this rigid glass/SU8 microchannel is higher than the highest used in the PDMS microfluidic systems (up to 100 µL/min).

Considering the relatively small electrode surface area (420 µm x 12.5 µm) in the systems mentioned above, we increased the electrode surface area 200 times (Fig.S7) and positioned them both perpendicular and parallel to the flow direction.

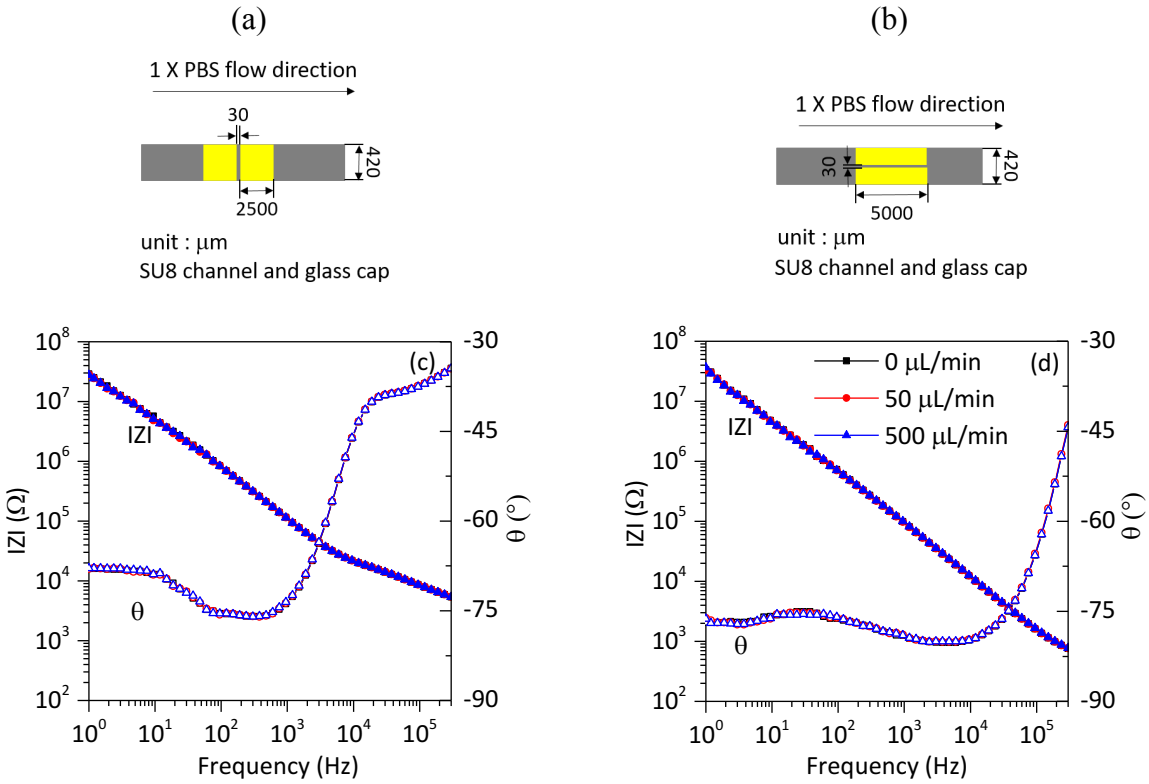

Figure S6. A pair of electrodes, used for impedance measurements, positioned perpendicular (a) and parallel (b) to the direction of the flow. (c) and (d) are the corresponding electrical complex impedances of 1X PBS solution vs. frequency under flow rates of 0 µL/min – black square, 50 µL/min – red round and 500 µL/min – blue triangle.

Figure S6 shows the electrical impedance of 1X PBS at flow rates of 0, 50 and 500 µL/min measured on electrodes pairs placed within rigid SU8 microchannels. No changes in electrical impedance were observed with increase in flow rate. These results demonstrate that in flexible PDMS microfluidic systems, the flow-induced drop in electrical impedance is strongly associated with the microchannel deformation.

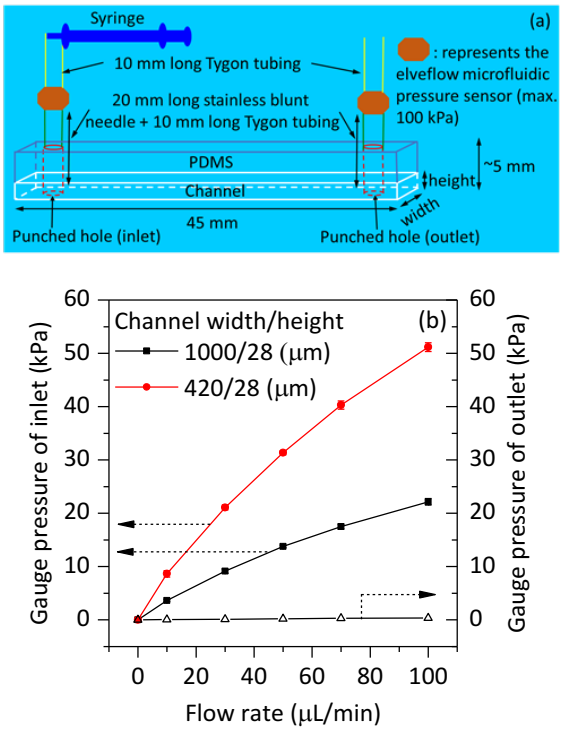

Figure S7. Gauge pressure measured at the inlet and outlet as a function of flow rate. (a) The schematic drawing of the system used for the measurement of inlet pressure. (b) The change of inlet and outlet pressures with the change of the volumetric flow rate of 1X PBS measured in PDMS microchannels of 45 mm long, 1000 μm or 420 μm wide and 28 μm high. To simplify the measurements, the pressure at the hub of the stainless steel needles (specifically locations outside the microchannel rather than within the microchannel) was considered to be the inlet and outlet pressure.

Figure S7 shows the variation in gauge pressure at the inlet and outlet with changes in fluid flow rates using 1X PBS in PDMS microchannels with dimensions of 45 mm long, 1,000 μm or 420 μm wide and 28 μm high. The inlet pressure increases from 0 kPa to approx. 20 kPa for 1,000 μm wide channels, and from 0 kPa to 50 kPa for 420 μm wide channels when, in both cases, the flow rate was increased from 0 μL/min to 100 μL/min. Interestingly, the increasing rate (i.e. slope of the curve) gradually decreases with the increase in flow rate, which is very similar to the relation between cross-sectional area and flow rate (Figure S5).

When measuring the outlet gauge pressure, the readout of the pressure sensor was found to be zero under flow rate changes going from 0 to 100 μL/min in both microchannels. We believe this is due to the extremely small outlet pressures (close to zero), which are nearly out of the measurement resolution of our used pressure sensor (2% of the max. 100 kPa, i.e. 0.2 kPa). We roughly calculated the corresponding outlet pressure based on the variation in the cross-sectional area towards the outlet of the 420 μm wide microchannel with changes in fluid flow rate (Figure 4), and found that the pressure increased from 0 to 0.3 kPa when increasing the flow rate from 0 to 100 μL/min. The outlet pressure values in Figure S7 are 0, 0.05, 0.1, 0.2, 0.3 kPa for flow rates of 0, 10, 30, 50, 100 μL/min, respectively.

Table S1. The boundary conditions for 2D COMSOL simulation

Geometry of channel cross section (width / height)	Pressure	Modulus of the Material	Figures
30 μm / 28 μm	35 kPa	2.5 MPa	Figure 6(c)
100 μm / 28 μm	35 kPa	2.5 MPa	Figure 6(b)
420 μm / 28 μm	35 kPa	2.5 MPa	Figure 6(a) and S7(a)
420 μm / 28 μm	35 kPa	3.5 MPa	Figure S7(B)

The influence of the PDMS microchannel geometry and its elastic modulus on the pressure-driven microchannel deformation was simulated. Table S1 summarizes the simulation conditions, including the channel geometry, applied pressure and the elastic modulus of the PDMS material.

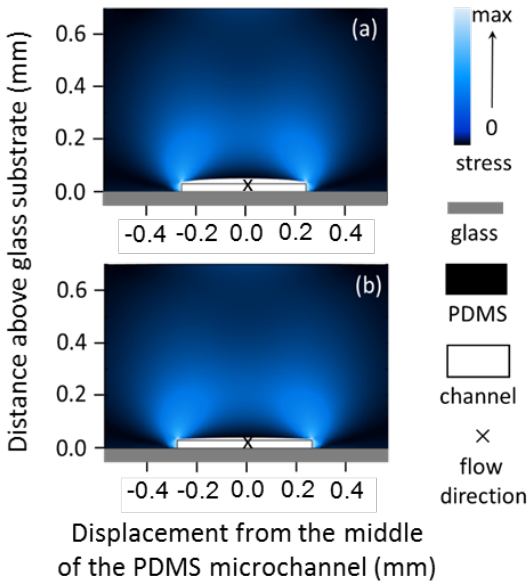

Figure S8. COMSOL simulation of stress field distribution in PDMS material with different elastic modulus. The channel width/height is 420/28 (μm). For the simulation, the applied pressure was 35 kPa and the elastic modulus were 2.5 MPa (a) and 3.5 MPa (b).

As shown in Fig.S8 (a) and (b), the pressure induced stress region extending into the PDMS material is the same for microchannels having the same geometry. But the bulging of the microchannel is less in harder materials, and is inversely proportional to the material modulus ($\varepsilon = \sigma/E, \varepsilon = strain, \sigma = stress, and\ E = modulus$). Therefore, using softer material would yield microfluidic devices with better sensitivity to flow rate. The stress regions extend as far out into the material as the dimension of the channel width.

Reference

Wang, Z., Volinsky, A. A., Gallant, N. D., *J. Appl. Polym. Sci.*, 2014, 131, 41050